

Review Article

IMPLEMENTATION OF NATURAL RANDOM FOREST MACHINE LEARNING METHODS ON MULTI SPECTRAL IMAGE COMPRESSION

¹k.Raju,²Sahitya Kiran Pilli, ³Gandi Siva Suresh Kumar, ^{*4}k saikumar, ⁵B.Omkar Lakshmi Jagan

¹Associate professor, dept. of ECE, narasaraopeta engineering college, Nrt, guntur, AP

²Assistant professor, dept. of ECE NS Raju Institute of Technology psahityakiran.ece@nsrit.edu.in

³Asst. professor, dept. of ECE, N S Raju Institute of Technology, sivasuresh.Ece@nsrit.edu.in

^{4*}Research scholar, dept. of ECE, KoneruLakshmaiah Education Foundation, Vaddeswaram, Guntur, Andhra Pradesh, India
saikumarkayam4@gmail.com

⁵Research Scholar, Department of Electrical and Electronics Engineering, KoneruLakshmaiah Education Foundation, Vaddeswaram, Guntur, Andhra Pradesh, India

Received: 05.10.2019

Revised: 15.11.2019

Accepted: 20.12.2019

Abstract:

Multispectral Image Compression (MSIC) is a current dominating challenge topic in research attention. Satellite communications, radars, sensing area technologies are continuously monitoring the earth, space and environment. In the competitive world resources, such as power, memory, and processing capacity are limitedly available. In this process multi spectral image processing techniques and methods requirement is very necessary like geographical information, optical information, disaster monitoring water wells etc.. So, Image quality compression, attacks, histogram equalization, machine learning statistical parameters need to be improve. Existing methods mainly based on matrix based modelling, DWT techniques segmentation methods, low rank tensor decomposition, but they are fail to discover the different strip components. Like, machine learning also did not solve the problems of spectral redundancy, sub bands removing models. In this research we are using natural random forest machine learning model (NRFML). This model compress and train the multi spectral image, at final comparing the parameters like MSE, PSNR, NCC, SSIM.

Keywords: Multi spectral Image, Natural random forest ML (NRFML), Spectral redundancy, sub bands removal.

© 2019 by Advance Scientific Research. This is an open-access article under the CC BY license (<http://creativecommons.org/licenses/by/4.0/>) DOI: <http://dx.doi.org/10.31838/jcr.06.05.42>

INTRODUCTION

Remote sensing technologies consist of different multispectral images (MI). These MI's consist of thousands of spectral bands (SPB) and sub bands (SB), we need to train this SPB, SB in a systematic manner. MI is very use full for many practical applications. Because of this spatial & spectral information is necessarily improved. Apart from sensing technologies, these MI's are inevitably generates from environment monitoring, military surveillance, urban planning devices etc. At that time generating MI's consist of different types of noises are added to spectral and spatial data. There are two types of remote image sensing technologies adjusted. i.e; Active image remote sensing and passive image remote image sensing. So Mean Square Error (MSE), peak Signal to Noise Ratio (PSNR), Normalized Correlation Coefficient (NCC) also very important parameters where the compression done. Until we analyse the PSNR, SSIM (Structural similarity) but Removal of Spectral Redundancy and removing sub-bands before compression concepts are not covered yet. These two parameters drastically reduce the memory (compression). So effective multispectral compression is achieved and PSNR, NCC, SSIM, MSE parameters are improved

Cameras are most generally utilized by every research organizations like DRDO, ISRO, in day by day life. This camera utilizes the different cluster to get the pictures from different sources. The channel permits single intensity cluster pixels at a time. The immovable picture in a camera is identified as an unfinished picture, which is additionally reproducing the captivated full-shading colors through the pipelined procedure, causes demosaicking. The extra utilized CFA is the Bayer CFA comprising of the green, red, blue pixels as well as paralleldrive. The Bayer example was created through Bayer [1] of the Eastman Kodak Corporation.

De_mosaicking [DMK] calculations contains heuristic & non-heuristic in environment. The heuristic methodology utilizes numerical figuring identified with demosaicking, and non-heuristic methodologies manage the short estimation of demosaicking calculations. The greater part of the DMK

calculations falls under the subsequent class (Figure 1). There is a few demand methods suggested on the CFA mosaic & DMK pictures. Protecting images are intended to disintegrate the repetitive pixel regard to histogram equalization. Image comprises of 2 sorts: Lossy as well as loss-less; the previous specific pixel data throughout model is feed backed with the help of machine learning techniques.

The programmable, interpixel, statically excess, and psychophysical redundancy has been compact with compression (comp) systems to reduce the no. of gray scale bits in an image (IMG). The proceedings in the designed knowledge have led to increase the neural network and fuzzy systems in all areas of research. There are a few developmental algorithms for powerful handling and distinguishing the ideal solutions. The nature-algorithm calculations are ongoing chain in advancement in neural systems, Fruit Fly Optimization [2], Particle swarm improvement [3], Gray Wolf Optimization calculation [4] and streamlining calculations. The proposed work outlines a Random Forest Optimization (RFO) calculation, which is effective in distinguishing the coefficients and finds the fittest function capacity. This enhancement have been prompt topassionate the induced methods through DMK to deliver a good outcome. The novel technique highlights the powerful reconstruction of a complete coloration photograph in mixture with the biorthogonal wavelet compression and optimizes the usage of RFO algorithm and Huffman Coding to attain higher compression coefficients in order that the reconstruction is more advantageous and the overall performance of the demosaicking process is improved.

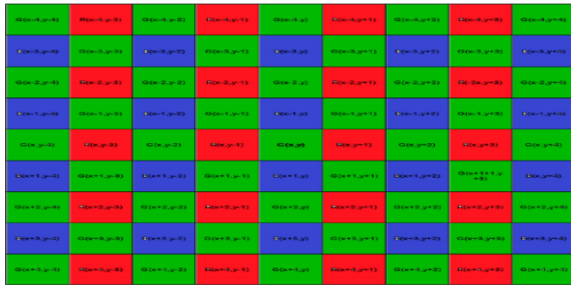


Figure: 1 RGB REPRESENTATION

Objectives

1. Image compression on satellite image
 2. Image quality assessment
 3. PSNR calculation
 4. MSE, SSIM, NCC Calculation
 5. Multispectral image compression such that calculating the compression ratio
 6. Different types of attacks
 7. Rotation attack
 8. Histogram equalization
 9. Colour improvement
 10. Mosaicking
- Step 2: Levers

Levers are the inputs that may be managed, or some modifications the Model may want to make, to force the objective described in step 1. For instance, to make certain that the customers are happy:

- A method can deliver unique blessings to existed model
- Give loose proposed version and design in a right manner

A device getting to know model can not be a lever, but it may help the organization choose out the levers. It's crucial to apprehend this distinction simply.

Step 3: Data

The subsequent step is to find out what statistics may be useful in figuring out and placing the lever that the business enterprise may additionally additionally have. This may be awesome from the statistics already supplied or amassed with the aid of the business enterprise in advance.

Step 4: Predictive fashions

Once we've the desired statistics that can be helpful in carrying out the above defined intention, the closing step is to build a simulation version in this facts. Note that a simulation model could have more than one predictive fashions. For instance, building one model figuring out what gadgets need to be recommended to a person, and every other model predicting the possibility that a person handle a particular parameter on a recommendation. The idea is to create an optimization version, as opposed to a predictive model.

A commonplace Characteristic of most multispectral images include neighbouring pixels, they're correlated. Such that exists redundant records. Redundancy and irrelevancy reductions are two essential components of compression.

a) Redundancy Reduction:

This is the method removing duplicate information of image from source.

b) Irrelevancy Reduction:

LITERATURE SURVEY

Satellite imaging has its spectrum of utilizations that ranges from earth observation, scientific research, military applications, natural resource management, global environmental monitoring and to the countless of applications. The acquisition of these images is done through

remote sensing sensor located from the satellites. It captures the earth with different wavelength and produce large amount of information in the form of different bands. The Multi-Spectral Scanner (MSS) produces the four bands of data, the Thematic Mapper (TM) designed to acquire image with seven bands and the High Resolution Imaging Spectrometer (HIRIS) produces the data with 192 bands [1]. These images are need to archived for learning and further processing with many applications [2]. The archiving and transmission of multispectral image is not the easy task because of the size factor. Hence, it need more amount of memory space and high bandwidth range for storage and transmission respectively due to its high degree of carrying information. Many approaches are proposed for compressing multispectral image. A vector quantization based methods [3,4], adopts the block based coding techniques in which blocks are operated in spatial domain and a non-linear block prediction is used to feat the spectral correlation. Another lossless method called Mean-normalized vector quantization is also proposed for compressing multispectral images [5]. An extended vector quantization based method that represents the 3-dimensional block using Kronecker Product with smaller vectors is proposed in [6]. In spite of these approaches, transform based methods are very effective with multispectral images [7]. A compression algorithm used Eigenregion-based Eigensubspace transform (ER-EST) [8] for multispectral images which is worked based on the decision rule that derived using principal correlation of an image correlation matrix. Then the eigen regions are classified using the decision rule and the eigen regions are compressed using ER- EST. A quadtree-based KLT transform [9] and wavelet based approaches on 3D domain [10,11] are also proposed for multispectral images. With this literature study, we can conclude that the wavelet based methods paves the way to efficient multispectral image compression especially with the 3D domain. Moreover, these methods may be irreversible and yield better compression performance [12,13]. As quality is the main aspect in the multispectral images, an optimal compression codec is needed that preserve the both compression and quality factors. Hence, in this paper, we proposed a near lossless multispectral image compression method that uses the Three-Dimensional Discrete Wavelet Transform (3D-DWT) and Huffman coding for encoding wavelet frequency coefficients. The remaining of this paper is organized as follows: Section 2 describes the necessary background knowledge for our proposed method. The methodology and working principle of our proposed method is illustrated in section 3, section 4 contains the evaluated results & discussion and finally we concluded the paper in section 5.

Organization of Paper

This paper finally divided into 8 sections, section-1 explains about introduction of colour filter array and different available algorithms. Section-2 deals about related work until accomplished achievements, section-3 explains about proposed random forest optimizations. Section-4 to 7 explains about different methods in the part of RFO and finally at section-8 explains about result and conclusion.

RELATED WORK

PSO:

PSO calculation has gotten wide consideration as of late. Favourable circumstances of PSO calculation can be explained as follow:

- (1) It has incredible strength and can be utilized in various application conditions with diminutive investigations
- (2) It has a solid conveyed capacity in radiance of the probability calculation is basically the swarm developmental calculation, so it is anything but difficult to acknowledge the parallel calculation.
- (3) It can merge to the streamline the functionality rapidly.
- (4) It is anything but difficult to analyze with different calculations to improve its exhibition

GA

This work similarly round the GA improvement of weighted/vector/directional/filters/(WVDF) [3], separating and upgrade the requests. The WVDF reorganization issue utilizing the numerical methodologies in [3]it has been demonstrated that these strategies can't combine to an all-around ideal weight vector. This can bring about more inaccurate WVDF saving qualities. Since the GA look through the entire arrangement space, they frequently give the all-around ideal arrangement.

GWO

Enhancing the image quality is a vital phase in each image processing scheme. The objective is to develop both the visual and the informational quality of distorted images. Contrast enhancement and brightness preservation are essential constraints for many vision based application. Histogram equalization (HE) fails to preserve the brightness while increasing the compare due to the unexpected mean shift throughout the procedure of equalization. To overcome the deficiency, intelligent approaches are applied for searching a new set of gray levels in such a way to achieve optimum image quality. In this methodology, Grey Wolf Optimization (GWO) algorithm is applied as an optimizer to extract the new usual of gray stages of the input image in the search space. The objective is to maximize the quality of the image by replacing the existing gray levels with new set of grey levels having reduced entropy and number of edges. Careful edge detector is applied to evaluate the image quality, entropy and number of edges in every possible solution. projected approach is tested on low contrast satellite images which give better performance in terms of PSNR, MSE.

PROPOSED WORK

This work is classified into 3 phases in first phase using random forest optimization classifying the trees. This trees explains how many code word required for processing. In phase two we are picking number of trees and original image for RFO-HOI for DMK. In phase three finally removing the de mosaicking and calculating PSNR, MSE, NCC

problem identification:

Above all methods mentioned in the section 2 are not suitable for removing the mosaicking so here we introduced new DMK model with the help of RFO algorithm. The existing methods like genetic algorithm it is a heuristic method of searching in AI. The computational steps and evaluation procedure for large data is complex. DE is a continuous traditional cross over implementation only for linear operations, random operations it does not handle efficiently, PSO algorithm is an intelligence procedure for strong coupling and complicated linear problems. Available optimization techniques are facing efficiency and quality of parameters like PSNR, SSIM, MSE, NCD etc. Using RFO these all limitations has been overcome because this is a machine learning model. Conventional model like [1] are not supporting DMK and denoising, so modern technologies support is necessary. The proposed system executes the CFA demosaicking with a successful wavelet transformation alongside the cutting edge RFO [6]. Fig/2 describes the diagram of the recommended work. There are systems that include errors on the DMK images, the investigated procedure are utilized before demosaicking, which creates enhanced DMK outcomes differ than ordinary calculations

The IMG is routing into High Pass as well as the Low Pass channels. The edges consume a great recurrence and even distributions can take low-recurrence coefficients. The importance of the coefficients assistances is recognizing the boundaries in the wavelet domain [8] (Figure 3) the investigated work has a "loss-less compression method" (LLCM) through bi-orthogonal wavelet change. A single scaling capacity is displaced by II scaling capacities in bi-orthogonal (BO) wavelet change. The control is focused on just a couple of the coefficients. BO wavelet gives additional level

of opportunity than added orthonormal changes. Estimates value residue in a base range also the element of the RFO that are hold & protected the IMG. Fig-4 portrays the vertical, out of line also even coefficient feature of the IMG on relating the BO wavelet change on behalf of picture comp. The massive measure of constants is finished, compression to be proficient. The filter coefficients are optimized using RFO.

RFO: This belongs to RFO chain related model.

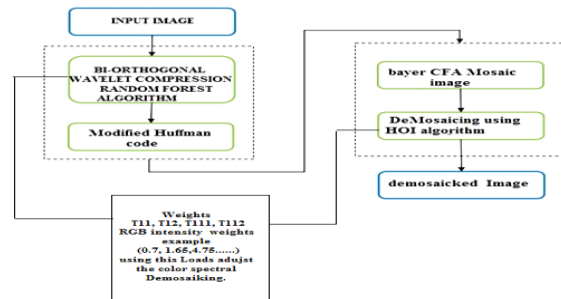


Figure: 2 DMKG with the help of RFO

Fig.2 explains that complete DMKG model, using random forest adjust the bi orthogonal wavelet compression. Input is the original image; this image is applied to training model here compression is performed for Image compression is a technique to reduce redundancy and irrelevancy of image data to enable its efficient transmission

PHASE-1

RFO is a responsive, easy-to-use ML approximation that generates an enormous result most frequently, though without super-parameter tuning. It is also one of probable most common analyses as it is straight-forward manner it can be used very well for arrangements also degeneration activities. RFO is an estimation of ML. The "forest" builds an outfit function of Decision Trees, ready with the suggested method. The general idea of the suggested method is that a mixture of learning models will build the overall result. Irregular RFO produce and assemble countless trees of choice in order to obtain a more accurate as well as stable predictions [9]. One significant chosen location of even direction is could be used very well for both exchange as well as disallow problems like AI frameworks. Here will address an arbitrary grouping of trees as the characterization is from time to time estimate AI's structure. Below we will see how trees might appear like a shifting Random Forest hyper-variable corresponding to a tree of selection. Fortunately, should not enter a tree choice with a recommended classifier and might simplest use the Random Forest classifier effectively. As we cited in advance, may additionally deal with Regression tasks use of the Random Forest regression. In creating the trees, Arbitrary Forest contributes extra randomness to the version. It scans for the exceptional overview amongst an uneven subset of characteristics in place of looking for the maximum very important factor while dividing a hub [10-12]. These effects are supplied in a wide at the side of a few varieties that consequences in an advanced version by using and massive. In Random Forest, such break, arbitrary subset of capabilities is considered by using dimension of centre. Creating trees means increasingly more abnormal with the help of arbitrary edges rather than attempting to find the maximum best edges for every element.

$$[CA, CH, CV, CD] = \text{dwt2}(X, 'sym4', 'mode', 'per') \text{-----} (1)$$

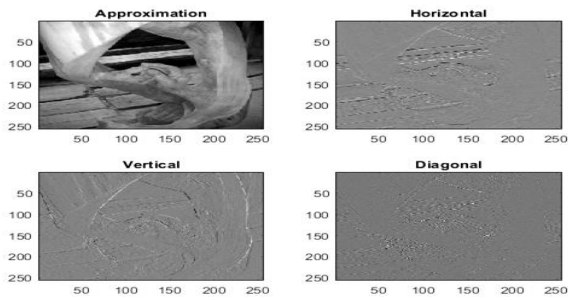


Figure: 3.Bi-orthogonal wavelet convert of level 1 as well as level 2 horizontal, diagonal also vertical detailed sub-images.

RFO-HOI ALGORITHM

In phase-2 RFO-HOI optimization is applied to decoded image& RFO have been applied at second stage, in first stage we are classifying required number trees, coming to second stage we need to apply higher order interest method on image. This one gives fitness function details like alpha beta and gama parameters. Finally HOI removes the demosacking and give full RGB values information [13-15].

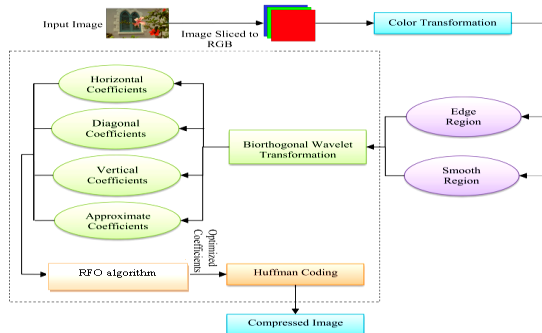


Figure: 4 optimized structure using RFO AND Huffman coding

The fig 4 explains that the overall random forest optimization for selected input image. In first step mosaic image has input tends to RGB slices and colour transformation has been performed with averaging the red, green, blue pixels. The forward step divided into two categories first one is edge region training second is smooth region training. With re-join mechanism combine the overall image, in fourth step wavelet transformation with bi-orthogonal mechanism has been used for diagonal, vertical, horizontal coefficients. At this stage obtain number of nodes for RFO, weights, trees had been decided. After RFO with the help of Huffman coding the image is compressed for storage or transmitting purpose, which is embedded image.

Random forests (RF-HOI) build numerous individual choices of trees at set up. Calculations are originated the all trees remain combined to create the last probability; the method of the classes for order or the mean probability is set back. As they utilize a gathering of outcomes to settle on an official choice, they are allowed as group systems.

HOI Node Data

$$ni_j = w_j C_j - w_{left(j)} C_{left(j)} - w_{right(j)} C_{right(j)} \quad (2)$$

Hoi significance is determined as the reduction in centre defect weighted by the possibility of arriving at that main node. The RF mechanism possibility field is determined via binary of assessments that arrive at the focus, isolated through way of the absolute quantity of tests. The complex fitness significance of extra considerable element.

$$ni_{sub(j)} = \text{the position of node } j \quad (3)$$

- $w_{sub(j)}$ = weighted amount of samples reaching node j
- $C_{sub(j)}$ = the impurity value of node j
- $left(j)$ = child node starting left split on node j
- $right(j)$ = child node from right split on node j

The significance aimed at every feature on a judgment tree is formerly considered as: hoi fitness function

$$fi_i = \frac{\sum_{j: \text{node } j \text{ splits on feature } i} ni_j}{\sum_{k \in \text{all nodes}} ni_k}$$

(4)

➤ $fi_{sub(i)}$ = the significance of feature i

➤ $ni_{sub(j)}$ = the significance of node j

$$normfi_i = \frac{fi_i}{\sum_{j \in \text{all features}} fi_j} \quad (5)$$

These would formerly stay able to be standardized to an incentive somewhere in the range of 0 as well as 1 by partitioning through the whole of all component significance esteems: The last include significance, at the Random Forest glassy, it's normal concluded every one of the trees. The aggregate of the component's significance esteem on every tree is determined also isolated through the absolute digit of trees:

$$RFfi_i = \frac{\sum_{j \in \text{all trees}} normfi_{ij}}{T} \quad (6)$$

➤ $RFfi_{sub(i)}$ = the significance of feature deliberate commencing entire trees in the Random Forest model

➤ $normfi_{sub(ij)}$ = the regularised feature reputation for i in tree j

➤ T = overall digit of trees

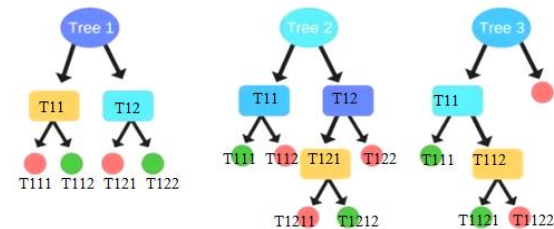


Figure: 5 decision tree diagram

Fig .5 explains about trees structure in this typical representation of squares denotes decision nodes and circles represents chance of nodes at final triangle represents the end nodes [4] Here T11, T12, T111, T112, etc are for classification of data and prediction of weights. Where each node attribute the test value, branch represents outcome of investigation and leaf node denotes a class label. The main Th value is calculated using `get red()`, `get green ()`, `get blue()`; commands average the each colour sample at final perform mean of three elements gives the threshold weight using this compare the T11, T12 etc. if Th is less than weight of node estimate as false operation otherwise it is an true estimation. This type of classification give the more accuracy compares conventional methods.

Arbitrary feedbacks are essentially an accumulation of unconventional trees whose outcomes are cumulative into one last outcome. Their capacity to constrain over fitting without significantly expanding mistake because of tendency is the reason they are such remarkable models. One way RFO difference is via preparing on various examples of the data [16-18].

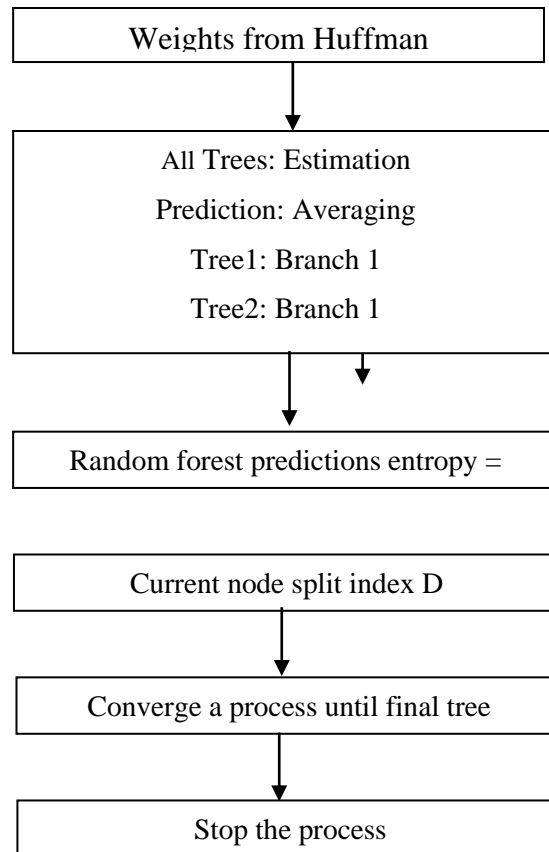


Figure :6 predicts solution in RFO

The above figure.6 shows that predictions assignment for trees and nodes, at this stage collect the entropy values from huffman method, also calculate the probability of each using estimation of statistical method. All trees are estimated using RFO mechanism, but number of branches are decided by using average prediction weight method. The overall random entropy is calculated by using entropy mathematical equation, D gives the current nodes splittings by help of Pi & D1, Dr nuemarics. The final random forest classification is performed until tree branches reach to zero positions. Stop the regression and prediction calculated the parameters like PSNR, SSIM, CC etc.

OPERATIONAL STEPS OF PROPOSED WORK

Input: "Colour_Image" from Kodak Data_set

Output: Demosaick image

Phase_I: EMBEDDING FOR DEMOSAICKING

Input: "Colour Image"

Output: "Compressed version _demosaick_image"

Step_1 The image is decomposed into L_L, L_H, H_L, H_H sub-bands.

Step_2 A {bi_orthogonal}DWT is applied to the decomposed image.

Step_3 The estimated & wavelet coefficients are strong-minded by DWT

Step_4 The ideal "coefficients" are determined by the R_FO optimization algorithm

Step_5 The redundancy in the compacted image is reduced by Modified_Huffman_Encoding (MHE).

Step :6 compressed demosaick image

Phase_II: ORIGINAL IMAGE EXTRACTING

Input: "Compresses De-mosaickImage"

Output: "Decompressed Image"

Step_1 The idleness is reduced by "Modified_Huffman" Ccoding.

Step_2 An IDWT is applied to retrieve the "compressed image"

Step_3 inverse image acquisition method

Step_4 original Image

Phase_III CLASSIFICATION OF IMAGE

Input: "Decompressed_Image"

Output: Reassembled or "Demosaicked_Image"

Step_1 Convert the compressed image to the mosaic image by Inverse Bayer C_FA.

Step_2 Green Channel is demosaicked in four instructions by High-order demosaicking.

Step_3 Red_Blue channel is "demosaicked" by falling the "Laplacian_value".

Step_4 RFO classification and regression is performed.

Step_5 Stop the process

The images and their load weights (for example pixel esteems and the event) are designed in the successive request base point. The pixel through the most remarkable event consumes the slowest code term; also the pixels through the least event through the biggest code word. The repetition is diminished

through combination prospects of the pixels consuming the most negligible event iteratively awaiting just 2 probabilities remain left also the objective is attained [19-22]. The code words remain representing, pixel respect to acquire the condensed picture subsequent to relating the BO wavelet change. An entropy encoder is utilized to get the ideal code on behalf of the pixel also their events as in Equation/(12) (Fig./6).

$$\text{Entropy} = - \sum_s P(s) \log_2(s) \quad \text{--- (7)}$$

Where's is the event of the pixel value also $P(s)$ is the probability of s . A feedback wavelet change is connected & over the filled picture to get the DMK IMG. The image is recreated back to its unique structure as a compressed picture on behalf of prompting request DMK [23].

High-orders DMK

Demosaicking is the manner towards assessing the disappeared energy estimation of the rudimentary image pixel to a complete whole-shading IMG. The COMP picture is demosaicked by using a four-directional demosaicking over the central area additionally not beside the edges [24-27]. The image is remade through COMP photo obtained after the above technique. The picture is modified over to a mosaic with a purpose to demosaic the comp photograph to accumulate an advanced recreated photo with effective results. The demosaicking method is separated into inexperienced power appreciate DMK as properly as red/blue green compression de-mosaicking.

Green intensity value demosaicking

The most ideal inaccurate misplaced control histogram worth is ordered through the closest realized pixel estimation. The demosaicking is completed beside the boundaries also over the inside pixel organize X, Y , so as to get progressively exact, estimation behalf of de-mosaicking. The great-request of subordinate is assessed by utilizing the Taylor arrangement [28-29] with the end goal that the misplaced green divert is recognized in the focused blue pixel area.

$$g(x, y) = \sum_{mn=0}^{\infty} \frac{g^{mn}(i, j)}{mn!} (x, y) - (i, j)^{mn} \quad \text{--- (8)}$$

A important dissimilarity approximation is exploited, somewhere

$$g'(x, y) = \frac{g(x, y+1) - g(x, y-1)}{2} \quad \text{--- (9)}$$

The 2nd order-derivative is attained by Equation as

$$\begin{aligned} \hat{G}_{x,y} &= G_{x,y-1} + g'(x, y-1) + \frac{1}{8}(g(x, y+1) \\ &\quad - 2g(x, y-1) + g(x, y-3)) \end{aligned} \quad \text{--- (10)}$$

$$\begin{aligned} \hat{G}_{x,y} &= G_{x,y-1} + \frac{1}{2}(B_{x,y} - B_{x,y-2}) + \frac{1}{8}(\hat{G}_{x,y+1} \\ &\quad - 2\hat{G}_{x,y-1} + \hat{G}_{x,y-3}) \end{aligned} \quad \text{--- (11)}$$

Where,

$$g'(x, y-1) = \frac{B_{x,y} - B_{x,y-2}}{2} \quad \text{--- (12)}$$

The pixel is extra isolated starting of the objective randomness is allotted with Loads of the maximum random pixel [10] decreasing, further to increment hundreds of the

closest intensity binary sample. It supplies an advanced determination beside the edge. The inexperienced compress DMK is scientifically communicated via Equations: -- 8 to twelve.

$$\begin{aligned} \hat{G}_{x,y}^N &= G_{x-1,y} + \frac{1}{2}(B_{x,y} - B_{x-2,y}) + \frac{1}{8}(G_{x+1,y} \\ &\quad - 2G_{x-1,y} + G_{x-3,y}) \end{aligned} \quad \text{--- (13)}$$

$$\begin{aligned} \hat{G}_{x,y}^S &= G_{x+1,y} + \frac{1}{2}(B_{x,y} - B_{x+2,y}) + \frac{1}{8}(G_{x-1,y} \\ &\quad - 2G_{x+1,y} + G_{x+3,y}) \end{aligned} \quad \text{--- (14)}$$

$$\begin{aligned} \hat{G}_{x,y}^E &= G_{x,y+1} + \frac{1}{2}(B_{x,y} - B_{x,y+2}) + \frac{1}{8}(G_{x,y-1} \\ &\quad - 2G_{x,y+1} + G_{x,y+3}) \end{aligned} \quad \text{--- (15)}$$

$$\begin{aligned} \hat{G}_{x,y}^W &= G_{x,y-1} + \frac{1}{2}(B_{x,y} - B_{x,y-2}) + \frac{1}{8}(G_{x,y+1} \\ &\quad - 2G_{x,y-1} + G_{x,y-3}) \end{aligned} \quad \text{--- (16)}$$

The above conditions are gotten from the critical estimation of the green force an incentive in IV ways (N, S, E, and W).

Red/blue intensity value DMK

The main demand analyse is aim & utilization at the red as well as blue force value DMK though the elevated-request test is utilized on behalf of the green power value demosaicking. The red also the blue power significance is tested to a huge degree also the precision can't be enhanced additional through high-request DMK. The De-mosaicking is evaluated in eight ways on behalf of the red/blue DMK. The red pixel force is an inducement in the blue and green areas in addition to blue an incentive in the red as well as green areas remain illustrious through Equations (22)- (29).

$$\begin{aligned} \hat{Rd}_{x,y-1}^N &= Rd_{x-1,y-1} + (Gr_{x,y-1} - \hat{Gr}_{x-1,y-1}) \\ \hat{Rd}_{x,y-1}^S &= Rd_{x+1,y-1} + (Gr_{x,y-1} - \hat{Gr}_{x+1,y-1}) \end{aligned} \quad \text{--- (17)}$$

The transparency conditions remain repeat on behalf of the blue power an incentive in the green as well as red areas of the picture. On adding the III force appreciation independently subsequently pressure, a totally DE-mosaicked pictures on behalf of the 3 power reorganization remains achieved [30-31].

$$\begin{aligned} \hat{Rd}_{x,y}^{NW} &= Rd_{x-1,y-1} + (\hat{Gr}_{x,y} - \hat{Gr}_{x-1,y-1}) \\ \hat{Rd}_{x,y}^{NE} &= Rd_{x-1,y+1} + (\hat{Gr}_{x,y} - \hat{Gr}_{x-1,y+1}) \\ \hat{Rd}_{x,y}^{SW} &= Rd_{x+1,y-1} + (\hat{Gr}_{x,y} - \hat{Gr}_{x+1,y-1}) \\ \hat{Rd}_{x,y}^{SE} &= Rd_{x+1,y+1} + (\hat{Gr}_{x,y} - \hat{Gr}_{x+1,y+1}) \end{aligned} \quad \text{--- (18)}$$

$$\hat{R}d_{xy-1}^E = Rd_{xy} + (Gr_{xy-1} - \hat{G}r_{xy})$$

$$\hat{R}d_{xy-1}^W = Rd_{xy-2} + (Gr_{xy-1} - \hat{G}r_{xy-2}) \quad \text{----- (19)}$$

On behalf of the test pictures, a "sliding window" completed a scope of interpretations in addition to scales is connected. Another sub-picture WI characterization by thinking about the normal of the probabilities $P_t, l(Y(I) = c)$:

$$\hat{Y}(I) = \arg \max_c \frac{1}{T} \sum_{t=1}^T P_{t,l}(Y(I) = c) \quad \text{----- (20)}$$

Wherever l is the sheet come through picture I in tree t . We group a picture I as the class C_k given through the R.O.I which provides the most elevated likelihood.

$$K(x, y) = \alpha K_A(x_{App}, y_{App}) + \beta K_S(x_{Shp}, y_{Shp}) \quad \text{----- (21)}$$

Equation 20 and 21 explains that rest classification weights. Here alpha and beta are weights.

RESULTS

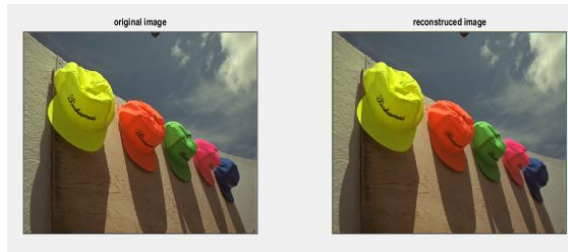


Figure: 7 originalvs. reconstruction images

Fig.7 shows that DMK of proposed method output here 1st one is original image and 2nd is RFO output image using proposed trees we achieve the good improvement



Figure: 8 demosaicking image

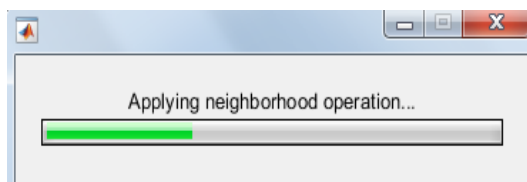


Figure: 9.Processing using RFO

Fig.8 & 9 explains that demosaicking processing and output of RFO based on proposed tree architecture here we got best clarity image by applying true tree on each iteration

Cmapclmax = 2 mmax = 2 nmax = 2 depthmax = 2

Subscripted assignment dimension mismatch.

Error in cmap (line 53) PQ(m,:)=parent.PQ;

>>branch

Error using branch (line 15)

Not enough input arguments.

>>cmapclmax = 5 mmax= 10nmax = 100 depthmax=20

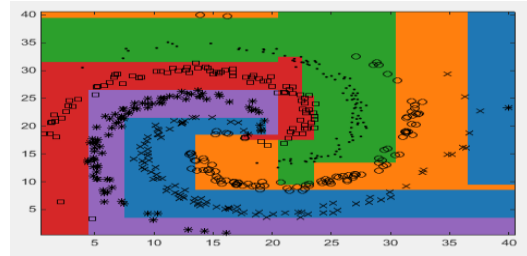


Figure: 10 Random Forest Pixels Pointing

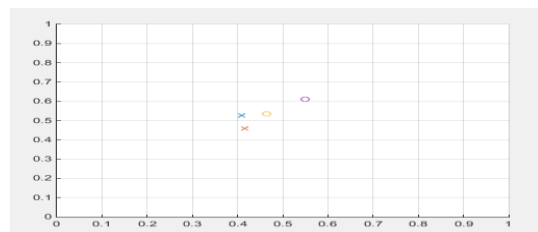


Figure: 11 pixels fixing in Matlab window

Fig.10.11 shows that pointing random image on proposed iteration here 2nd figure explains that tree true or false classification based on random search.

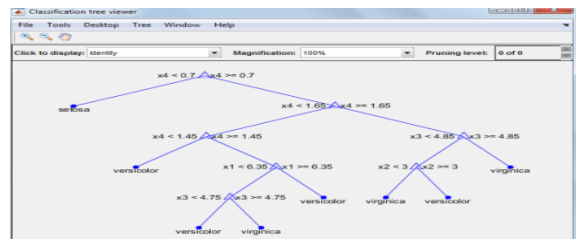


Figure: 12 tree representation

Fig.12.explains that depending upon tree value gave the false or true justification on data base images

Tree Bagger

Collaborativethrough 60 bagged choiceof trees:

Training/X: [150x4]

Training/Y: [150x1]

Method:- classification

Nvars: 4

NVarToSample :2

MinLeaf: 1

FBoot: 1

SampleWithReplacement: 1

ComputeOOBPrediction : 1

ComputeOOBVarImp:

Proximity:[] Class Names: 'setosa' 'versicolor' 'virginica'

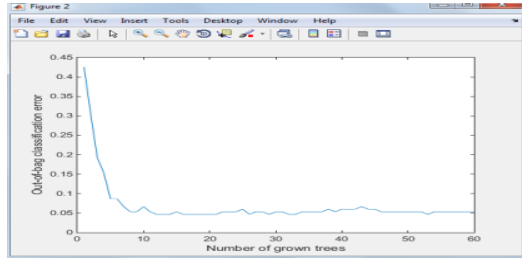


Figure: 13 trees classification

Table: 1MSE PSNR NCD values comparison $p_v=0.05$

METHODS	GA			(PPPSO)			GWO		
	PSNR	MSE	NCD	PSNR	MSE	NCC	PSNR	MSE	NCC
Noisy	0.99	427.3	0.0445	27	996.9378	0.4894	-	-	-
MF	9.23	49.7	0.0442	27.9	45.4913	0.0485	-	-	-
VMF	2.56	50.8	0.0403	28.32	46.4913	0.0464	-	-	-
BVDF	2.35	58.6	0.0407	38.48	91.8953	0.0537	-	-	-
GVDF	5.32	55.3	0.0420	39.42	-	-	-	-	-
SMF	6.35	45.6	0.0406	40.32	-	-	29.6322 (D2)	29.6322 (D2)	0.9391 (D2)
LWVDF	7.36	33.4	0.0256	41.36	62.0878	0.0445	22.4328 (C2)	22.4328 (C2)	0.9406 (C2)
SWVDF	8.32	24.2	0.0188	47.32	62.0878	0.0445	28.7643 (B2)	28.7643 (B2)	0.9138 (B2)
Proposed	9.480	24.8	0.0113	58.32	0.0076	0.0011	36.8721 (A2)	18.2945 (A2)	0.9581 (A2)

Table: 2 RFO values comparison

Image	RFO		
	PSNR	MSE	NCD
GA	9.480	24.8	0.0113
PPPSO	58.32	0.0076	0.0011
GWO	36.8721	18.2945	0.9581
RFO	60.02	0.0062	0.9987

Table .1 ,2 explains that proposed method got fewer mean square error as fineasgreathighest to signal noise ratio based on this clearly said that random forest optimization is good method in analysis of demosaicking[31-35]

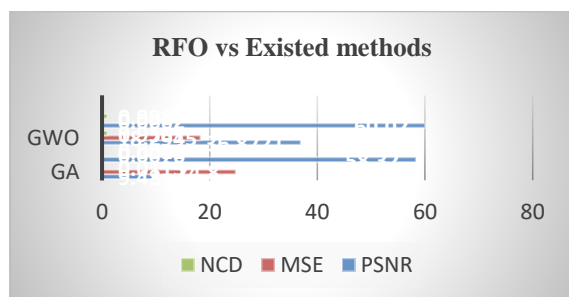


Figure: 14 comparison of methods

Fig.14 explains about comparison all method like RFO, GWO, PPPSO, GA all methods are compared with NCD, PSNR, MSE values.

CONCLUSION

Finally conclude that using CFA along genetic algorithm, particle swarm optimization, gray wolf optimization gives less

efficiency and PSNR, MSE, NCD these values are not accuratefor analysis, compared to existed methods, proposed method that is CFA with random forest optimization is better accurate and NCD Here attain the PSNR=60.02 this is an good achievement, MSE=0.0062 that means very less error, normalized colour difference NCD is very nearer to one. So at last discussed about mosacking, this effect is inconvenience, related to colour quality of image. This nature is trained and removed by using Random forest optimization method finally obtain the Demosaik image with better auality.

REFERENCES

1. Bayer BE. Color imaging array. United States Patent 3,971,065. 1976.
2. Xing B, Gao W-J. Fruit Fly optimization algorithm innovative computational intelligence. A rough guide to 134 clever algorithms. IntellSyst Ref Libr. 2014;62:167–170. DOI:10.1007/978-3-319 03404-1.
3. Wang D, Tan D, Liu L. Particle swarm optimization algorithm : an overview. Soft Comput. 2017. DOI:10.1007/ s00500-016-2474-6.
4. Mirjalili S, Mohammad S, Lewis A. Grey wolf optimizer. AdvEngSoftw. 2014;69:46–61. DOI:10.1016/j.advengsoft. 2013.12.007.
5. Li JS, Randhawa S. Color filter array demosaicking using high-order interpolation techniques with a weighted median filter for sharp color edge preservation. IEEE

- Trans Image Process. 2009;18:1946–1957. DOI:10.1109/TIP.2009.2022291.
6. R. Lukac, B. Smolka, K.N. Plataniotis, and A.N. Venetsanopoulos, "Selection weighted vector directional filters," Computer Vision and Image Understanding, Special Issue on Colour for Image Indexing and Retrieval, to appear, 2004.
7. Pekkuksen I, Altunbasak Y. Gradient based threshold free color filter array interpolation, in: international conference on image processing. ICIP. 2010: 137–140. DOI:10.1109/ICIP.2010.5654327.
8. Pekkuksen I, Altunbasak Y. Multiscale gradients based color filter array interpolation. IEEE Trans Image Process. 2013;22:157–165. DOI:10.1109/TIP.2012.2210726.
9. He L, Chen X, Jeon G, et al. Improved directional weighted interpolation method for single-sensor camera imaging. Opt Eng. 2014;53:093103. DOI:10.1117/1.OE.53.9.093103.
10. Duran J, Buades A. Self-Similarity and spectral correlation adaptive algorithm for color demosaicking. IEEE Trans Image Process. 2014;23:4031–4040.
11. Chen X, Jeon G, Jeong J. Voting-Based directional interpolation method and Its application to still color image demosaicking. IEEE Trans Circuits Syst Video Technol. 2014;24:255–262. DOI:10.1109/TCSVT.2013.2255421.
12. Shi J, Wang C, Zhang S. Region-adaptive demosaicking with weighted values of multidirectional information. J Commun. 2014;9:930–936. DOI:10.12720/jcm.9.12.930-936.
13. Chang K, Ding PLK, Li B. Color image demosaicking using inter-channel correlation and nonlocal self-similarity. Signal Process Image Commun. 2015;39(Part A):264–279. DOI:10.1016/j.image.2015.10.003. Figure 10. Comparative analysis of the average FSIM values. THE IMAGING SCIENCE JOURNAL 9.
14. Kiku D, Monno Y, Tanaka M, et al. Minimized-Laplacian residual interpolation for color image demosaicking. Proceedings of SPIE-IS&T Electronic Imaging; 2014. DOI:10.1117/12.2038425.
15. Ye W, Ma KK. Color image demosaicking using iterative residual interpolation. IEEE Trans Image Process. 2015;24:5879–5891. DOI:10.1109/TIP.2015.2482899.
16. Kim Y, Jeong J. Four-Direction residual interpolation for demosaicking. IEEE Trans Circuits Syst Video Technol. 2016;26:881–890. DOI:10.1109/TCSVT.2015.2428552.
17. Jeon G, Anisetti M, Wang L, et al. Locally estimated heterogeneity property and its fuzzy filter application for deinterlacing. Inf Sci. 2016;354:112–130. DOI:10.1016/j.ins.2016.03.016.
18. Shao P, Ding S, Ma L, et al. Edge-preserving image decomposition via joint weighted least squares. Comput Vis Media. 2015;1:37–47. DOI:10.1007/s41095-015-0006-4.
19. Jia X, Zhao B, Zhou M, et al. An edge-adaptive demosaicking method based on image correlation. J Cent South Univ. 2015;22:1397–1404. DOI:10.1007/s11771-015-2657-9.
20. Chen X, He L, Jeon G, et al. Multidirectional weighted interpolation and refinement method for Bayer pattern CFA demosaicking. IEEE Trans Circuits Syst Video Technol. 2015;25:1271–1282. DOI:10.1109/TCSVT.2014.2313896.
21. Wu J, Anisetti M, Wu W, et al. Bayer demosaicking with polynomial interpolation. IEEE Trans Image Process. 2016;25:5369–5382. DOI:10.1109/TIP.2016.2604489.
22. Zhang C, Li Y, Wang J, et al. Universal demosaicking of color filter arrays. IEEE Trans Image Process. 2016;25:5173–5186. DOI:10.1109/TIP.2016.2601266.
23. Lien CY, Yang FJ, Chen PY. An efficient edge-based technique for color filter array demosaicking. IEEE Sens J. 2017;17:4067–4074. DOI:10.1109/JSEN.2017.2706086.
24. Li N, Li JSJ, Randhawa S. Color filter array demosaicking based on the distribution of directional color differences. IEEE Signal Process Lett. 2017;24:604–608. DOI:10.1109/LSP.2017.2658667.
25. Wang J, Wu J, Wu Z, et al. Bilateral filtering and directional differentiation for Bayer demosaicking. IEEE Sens J. 2017;17:726–734. DOI:10.1109/JSEN.2016.2623422.
26. Tan DS, Chen W-Y, Hua K-L. Deep demosaicking: adaptive image demosaicking via multiple deep fully convolutional networks. IEEE Trans Image Process. 2018;27:2408–2419. DOI:10.1109/TIP.2018.2803341.
27. Zhang N, Wu X. Lossless compression of color mosaic images. IEEE Trans Image Process. 2006;15:1379–1388.
28. Calderbank AR, Daubechies I, Sweldens W, et al. Wavelet transforms that Map integers to integers. Appl Comput Harmon Anal. 1998;5:332–369.
29. Tizhoosh HR. (2005). Opposition-based learning : a new scheme for machine intelligence, International Conference on Computational Intelligence for Modelling, Control and Automation, and International Conference on Intelligent Agents, Web Technologies and Internet Commerce.
30. Huffman DA. (1952). A method for the construction of minimum-redundancy codes, Proceedings of the I.R.E. A. p. 1098–1101.
31. Kreyszig E. (2006). Advanced engineering mathematics.
32. Ibrahim Pekkuksen YA. (2010). Gradient based threshold free color filter array interpolation. Proceedings of the IEEE International Conference of Image Processing. p. 137–140.
33. Kiku D, Monno Y, Tanaka M, et al. (2013). Residual Interpolation for Color Image Demosaicking. Proceedings of the International Conference on Image Processing. ICIP 2304–2308. DOI:10.1109/TIP.2016.2518082.
34. Kiku D, Monno Y, Tanaka M, et al. Beyond color difference: residual interpolation for color image demosaicking. IEEE Trans Image Process. 2016;25:10. DOI:10.1109/TIP.2016.2518082.
35. Prashant Tiwari, Puravi Nayak, Shakti Ketan Prusty, Pratap Kumar Sahu. "Phytochemistry and Pharmacology of *Tinospora cordifolia*: A Review." Systematic Reviews in Pharmacy 9.1 (2018), 70-78. Print. doi:10.5530/srp.2018.1.14
37. Mahalle, N., Kulkarni, M.V., Naik, S.S. Is hypomagnesaemia a coronary risk factor among Indians with coronary artery disease (2012) Journal of Cardiovascular Disease Research, 3 (4), pp. 280-286.
38. DOI: 10.4103/0975-3583.102698